

# Lifetimes and transition frequencies of several singlet *ungerade* states in N<sub>2</sub> between 106 000 and 109 000 cm<sup>-1</sup>

J.P. Sprengers\*, W. Ubachs

Laser Centre, Department of Physics and Astronomy, Vrije Universiteit, De Boelelaan 1081, 1081 HV Amsterdam, The Netherlands

Received 26 September 2005; in revised form 26 October 2005

Available online 15 December 2005

## Abstract

Using a narrow-band tunable XUV source, ultra-high resolution 1 XUV + 1 UV two-photon ionisation spectra were recorded of transitions to several singlet *ungerade* states in <sup>14</sup>N<sub>2</sub> and <sup>15</sup>N<sub>2</sub> in the range 106 000–109 000 cm<sup>-1</sup>. The natural linewidths of the individual rotational spectral lines were determined and the resulting lifetimes were found to depend on vibrational level and for the *c*<sub>3</sub><sup>1</sup>Π<sub>u</sub>(*v* = 1) level also on isotope. Furthermore, accurate transition frequencies were determined and for several bands, lines near bandhead regions were resolved for the first time.

© 2005 Elsevier Inc. All rights reserved.

**Keywords:** Molecular nitrogen; Extreme ultraviolet spectra; Predissociation

## 1. Introduction

The dipole-allowed transitions in molecular nitrogen from the ground state *X*<sup>1</sup>Σ<sub>g</sub><sup>+</sup>, accessing excited states of singlet *ungerade* symmetry (*c*<sub>4</sub><sup>1</sup>Σ<sub>u</sub><sup>+</sup>, *b*<sup>1</sup>Σ<sub>u</sub><sup>+</sup>, *c*<sub>3</sub><sup>1</sup>Π<sub>u</sub>, *o*<sup>1</sup>Π<sub>u</sub>, and *b*<sup>1</sup>Π<sub>u</sub>), lie in the extreme ultraviolet (XUV) spectral domain. Strong Rydberg–valence and rotational interactions perturb the structure and intensity distribution [1–3], while additional spin–orbit interactions with triplet *ungerade* states cause predissociation of the singlet states. A large number of linewidth and lifetime measurements (see [4] and references cited therein) show a predissociation rate strongly depending on vibrational level and isotope. Lewis et al. [5] explained the predissociation for the *b*<sup>1</sup>Π<sub>u</sub>(*v* = 0–6) and *c*<sub>3</sub><sup>1</sup>Π<sub>u</sub>(*v* = 0) states, lying in the energetic range 100 000–106 000 cm<sup>-1</sup>, in terms of interactions with the *C*<sup>3</sup>Π<sub>u</sub> and *C*<sup>3</sup>Π<sub>u</sub> states. To extend their theoretical predissociation model to higher singlet states, more information is required (and recently became available [6,7]) on the *F*<sup>3</sup>Π<sub>u</sub> and *G*<sup>3</sup>Π<sub>u</sub> states, which are supposed to play significant roles at higher energies [5]. Second, a

comprehensive set of linewidth and lifetime measurements on singlet *ungerade* states at these higher energies is required to give a detailed picture of the predissociation behaviour and to explain the underlying mechanisms. Recently, linewidth measurements of several singlet *ungerade* states in the region 109 000–112 000 cm<sup>-1</sup> were reported [8,9] and here we present new frequency domain linewidth measurements on the singlet *ungerade* states between 106 000 and 109 000 cm<sup>-1</sup>. The present ultra-high resolution 1 XUV + 1 UV two-photon ionisation spectra also yield accurate line positions and several lines near bandhead regions are resolved for the first time.

## 2. Experiment

This paper reports on an extension of previous experiments on linewidths in the N<sub>2</sub> spectra using the ultra-high resolution XUV laser in Amsterdam [4]. Now the system has been modified to produce XUV radiation at energies exceeding 106 000 cm<sup>-1</sup>. The extension has been documented before [10] and will only be briefly described here. The output of a narrow-band tunable cw ring dye laser, pumped by a 532-nm Millennia-V laser, was amplified in a pulsed dye amplifier (PDA), which was in turn pumped with the second

\* Corresponding author. Fax: +31 205987999.

E-mail address: arjan@nat.vu.nl (J.P. Sprengers).

harmonic of a pulsed Nd:YAG laser. The output of the PDA was mixed with a  $\sim 100$  mJ/pulse 532-nm green beam (15% from the same narrow-band injection-seeded Nd:YAG laser used to pump the PDA) in a KD\*P crystal to generate UV radiation with typical powers of 10–15 mJ/pulse. XUV radiation was produced by nonresonant frequency tripling the UV in a xenon gas jet obeying the following relation:  $\omega_{\text{XUV}} = 3\omega_{\text{PDA}} + 3\omega_{\text{Nd:YAG}}$ . Absolute frequency calibration of  $\omega_{\text{PDA}}$  was done by applying  $\text{I}_2$  saturation spectroscopy on the cw ring dye laser output, while relative calibration was achieved with an étalon. Calibration of  $\omega_{\text{Nd:YAG}}$  was performed with an ATOS wavemeter. The XUV beam was perpendicularly crossed with a skimmed  $\text{N}_2$  supersonic jet and the  $\text{N}_2^+$  ions formed in the 1 XUV + 1 UV ionisation scheme were accelerated to a electron-multiplier detector in a time-of-flight setup. A 99.40% isotopically enriched gas sample (Euriso-top) was used for the  $^{15}\text{N}_2$  measurements.

Philip et al. [10] deduced a XUV source bandwidth of 300 MHz at full width at half maximum (FWHM) (all further widths and bandwidths in this paper are FWHM) by measuring a long-lived krypton resonance at a nozzle–skimmer distance of 150 mm. This is the same bandwidth determined from measurements applying the third harmonic of the frequency-doubled output of the PDA corresponding to  $\omega_{\text{XUV}} = 6\omega_{\text{PDA}}$  [4]. For strong signal levels, a nozzle–skimmer distance of 150 mm was used also for the  $\text{N}_2$  studies, but for weaker lines, this distance was decreased resulting in extended Doppler broadening and less accurate measurements. In worst cases, the nozzle was located only a few millimeters before the skimmer to obtain a sufficient signal-to-noise ratio. In the subsequent data analysis, the same function of the instrument width against nozzle–skimmer distance as given in [4] was used, in which the XUV bandwidth is constant and the Doppler width depends on the nozzle–skimmer geometry.

### 3. Results

With the present setup, 1 XUV + 1 UV two-photon ionisation spectra were recorded, probing the  $b^1\Pi_u(v=10)$ ,  $c_3^1\Pi_u(v=1,2)$ ,  $c_4^1\Sigma_u^+(v=1,2)$ , and  $b^1\Sigma_u^+(v=4,6)$  states in  $^{14}\text{N}_2$  and the  $b^1\Pi_u(v=9)$ ,  $c_3^1\Pi_u(v=1)$ ,  $o^1\Pi_u(v=1)$ ,  $c_4^1\Sigma_u^+(v=1)$ , and  $b^1\Sigma_u^+(v=5,6)$  states in  $^{15}\text{N}_2$ . Examples of spectra are shown in Figs. 1 and 2 for the  $c_4^1\Sigma_u^+ - X^1\Sigma_g^+(2,0)$  and  $b^1\Pi_u - X^1\Sigma_g^+(10,0)$  bands, respectively. In Fig. 2 and its caption, the procedure is demonstrated to convert the online calibrated frequency  $\omega_{\text{PDA}}$  (scanned) and  $\omega_{\text{Nd:YAG}}$  (fixed) into a scale for the XUV frequencies. Not all levels in the energy range 106 000–109 000  $\text{cm}^{-1}$  are presented here because of several reasons. Raw data were obtained for  $b(9)$  and  $o(1)$  in  $^{14}\text{N}_2$ , but the strong mutual perturbation [11] requires further analysis before the lines can be assigned unambiguously and the predissociation behaviour presented. Also the  $c_3(1)$  level in  $^{15}\text{N}_2$  has local interactions but in this case with a triplet state [3] and here only a value of the lifetime

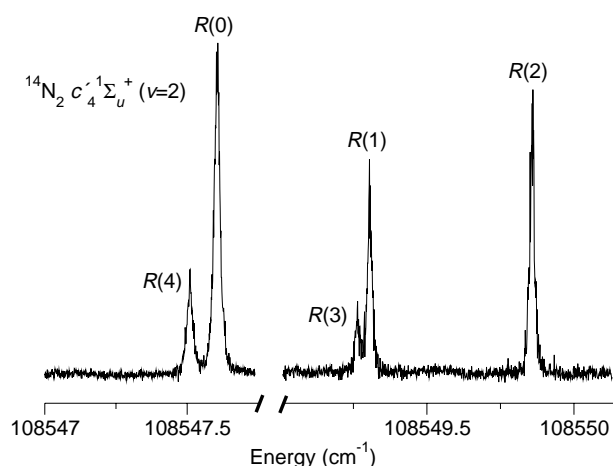


Fig. 1. 1 XUV + 1 UV ionisation spectrum for the  $^{14}\text{N}_2$   $c_4^1\Sigma_u^+ - X^1\Sigma_g^+(2,0)$  band. The  $R(0)$  and  $R(4)$  lines and the  $R(1-3)$  lines are resolved for the first time. Left spectrum is recorded with a smaller nozzle–skimmer distance than the spectrum at the right, i.e., the widths are slightly larger in the left spectrum due to increased Doppler broadening.

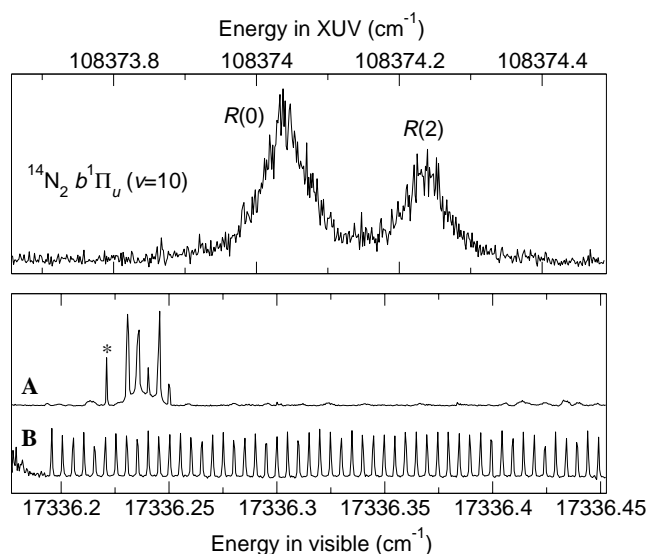


Fig. 2. Upper spectrum: 1 XUV + 1 UV ionisation spectrum for the  $^{14}\text{N}_2$   $b^1\Pi_u - X^1\Sigma_g^+(10,0)$  band. Nozzle–skimmer distance = 40 mm. The lines are lifetime broadened and clearly show a dominant Lorentzian contribution. The  $R(0)$  and  $R(2)$  lines are resolved for the first time. Lower spectrum: (A) Simultaneously recorded  $\text{I}_2$  saturation spectrum. The line marked with an asterisk is the “ $r$ ” hyperfine component of the  $B - X(19-2)$   $P56$  line of  $\text{I}_2$  at 17 336.22109  $\text{cm}^{-1}$ , used for absolute calibration of  $\omega_{\text{PDA}}$ . (B) Simultaneously recorded étalon markers for relative calibration of  $\omega_{\text{PDA}}$ . Three photons of the green beam, with an energy of  $\omega_{\text{Nd:YAG}} = 18788.3766$   $\text{cm}^{-1}$ , has to be added to obtain the frequency  $\omega_{\text{XUV}} = 3\omega_{\text{PDA}} + 3\omega_{\text{Nd:YAG}}$  shown in the upper curve.

is given, while a detailed analysis of the perturbations will be presented elsewhere. No signal levels corresponding to the transitions to  $b(8)$  in both  $^{14}\text{N}_2$  and  $^{15}\text{N}_2$  and  $b'(4)$  in  $^{15}\text{N}_2$  were detected, probably because of a lack of sufficient XUV power. We note here that in the present XUV-production scheme involving  $\omega_{\text{XUV}} = 3\omega_{\text{PDA}} + 3\omega_{\text{Nd:YAG}}$ , the XUV intensity is less than in the sextupling

( $\omega_{\text{XUV}} = 6\omega_{\text{PDA}}$ ) scheme [4]. Excited states  $b(10)$ ,  $c_3(2)$ , and  $c'_4(2)$  in  $^{15}\text{N}_2$  were not investigated because the energy positions of the bandheads are not known to sufficient accuracy to attempt an ultra-high resolution study; searching for these lines would consume too much expensive  $^{15}\text{N}_2$  gas. Finally,  $b'(5)$  in  $^{14}\text{N}_2$  was already presented in [10].

### 3.1. Line positions

The observed transition frequencies and assignments are tabulated for  $^{14}\text{N}_2$  and  $^{15}\text{N}_2$  in Tables 1 and 2, respectively. The absolute accuracy of the spectral measurements is estimated at  $\pm 0.01 \text{ cm}^{-1}$  [10], significantly larger than the accuracy of  $\pm 0.003 \text{ cm}^{-1}$  in our other studies on  $\text{N}_2$  [3,4]. The higher uncertainty is associated with the limited accuracy of the ATOS wavemeter and small drifts of  $\omega_{\text{Nd:YAG}}$  during the scans [10]. These estimates are for the narrower resonances, while for lines with a significant Doppler contribution or

Table 1  
Observed transition frequencies (in  $\text{cm}^{-1}$ ) in  $^{14}\text{N}_2$

Level	$J$	$R(J)$	$Q(J)$	$P(J)$		
$b^1\Pi_u(v=10)$	0	108374.040				
	1	108374.911	108370.063			
	2	108374.236	108366.956			
	3	108372.003				
	4	108368.199				
$c_3^1\Pi_u(v=1)$	0	106531.442				
	1	106534.334	106527.443			
	2		106526.323			
$c_3^1\Pi_u(v=2)$	0	108698.00				
	$c'_4^1\Sigma_u^+(v=1)$	0	106371.966			
		$c'_4^1\Sigma_u^+(v=2)$	0	108547.605		
			1	108549.305		
			2	108549.858		
3	108549.264					
$b^1\Sigma_u^+(v=4)$	4	108547.510				
	0	106649.145				
	1	106650.228				
	2	106649.903				
	$b^1\Sigma_u^+(v=6)$	0	108000.93*			
1				107994.49		
2		108000.93*		107988.94		
3		107998.65				
4		107994.73				
5	107989.23					

Lines marked with \* are blended lines in the spectrum. Lines given in less significant digits have undergone lifetime and/or Doppler broadening.

Table 2  
Observed transition frequencies (in  $\text{cm}^{-1}$ ) in  $^{15}\text{N}_2$

Level	$J$	$R(J)$	$Q(J)$
$b^1\Pi_u(v=9)$	1	107446.97	107442.34
$\sigma^1\Pi_u(v=1)$	1	107582.40	107575.92
$c'_4^1\Sigma_u^+(v=1)$	1	106313.887	
	$b^1\Sigma_u^+(v=5)$	0	107229.574
1		107230.200	
$b^1\Sigma_u^+(v=6)$	2	107229.284	
	1	107877.81	

Lines given in less significant digits have undergone lifetime and/or Doppler broadening.

lifetime broadening, a lower accuracy of  $\pm 0.02 \text{ cm}^{-1}$  is estimated. Note that the resolving power, i.e., bandwidth, of the setups with  $\omega_{\text{XUV}} = 3\omega_{\text{PDA}} + 3\omega_{\text{Nd:YAG}}$  and  $\omega_{\text{XUV}} = 6\omega_{\text{PDA}}$  are similar, notwithstanding the fact that the accuracies are different.

For most nozzle-skimmer geometries, a low rotational temperature in the gas expansion only allowed population of low rotational levels with  $J \leq 5$ . Near the  $R$ -branch bandheads regions, many individual lines were resolved for the first time. For example, the  $R(0)$  and  $R(4)$  and the  $R(1-3)$  of the  $c'_4 - X(2,0)$  band in  $^{14}\text{N}_2$  are clearly separated (see Fig. 1) and also the  $R(0)$  and  $R(2)$  lines of the  $b - X(10,0)$  band in  $^{14}\text{N}_2$  are resolved for the first time (see Fig. 2). These levels have all been measured and analyzed before with a lower resolution for  $^{14}\text{N}_2$  [12–17] and  $^{15}\text{N}_2$  [3]. To identify the resolved lines, transition frequencies were calculated from the known molecular constants. Since only a limited amount of lines were measured, no attempts were made to improve the molecular constants.

### 3.2. Linewidths

From the recorded 1 XUV + 1 UV ionisation spectra, linewidths for the individual rotational lines of all bands were determined using the same procedures and instrument function as in [4] to deconvolve the instrument function from the observed widths to obtain natural linewidths  $\Gamma$ . Subsequently, lifetimes were derived using  $\tau = 1/2\pi\Gamma$  and the results for the various states investigated are tabulated for both  $^{14}\text{N}_2$  and  $^{15}\text{N}_2$  in Table 3. For the small range of low  $J$  levels studied ( $J \leq 5$ ) no evidences of  $J$ -dependences were found. Also no differences in lifetime between  $\Pi^+$  or  $e$  parity levels (observed in  $R$  and  $P$  branches) and  $\Pi^-$  or  $f$  parity levels ( $Q$  branches) were observed, in the case of the  $^1\Pi_u$  states.

#### 3.2.1. $^1\Pi_u$ states

One vibrational level of the  $b^1\Pi_u$  state was investigated in  $^{14}\text{N}_2$ , namely  $b(10)$ , providing the first reported lifetime for this level of  $100 \pm 15 \text{ ps}$ . In  $^{15}\text{N}_2$ , the  $b(9)$  level was studied, yielding a lifetime of  $46 \pm 7 \text{ ps}$ . This value is only derived from several scans of the  $Q(1)$  line, corresponding to  $f$  symmetry levels. Because of a low signal-to-noise ratio, no accurate linewidths of  $R$  (and  $P$ ) lines were determined and hence, the present lifetime of  $b(9)$  in  $^{15}\text{N}_2$  applies to  $f$  parity levels only.

The  $c_3^1\Pi_u$  Rydberg state was studied for vibrational levels  $v = 1, 2$  in  $^{14}\text{N}_2$  and  $v = 1$  in  $^{15}\text{N}_2$ . A significant isotope dependence is found for  $c_3(1)$ , as shown in Fig. 3. Clearly lifetime broadened lines were observed in  $^{14}\text{N}_2$  giving a lifetime of  $155 \pm 30 \text{ ps}$ , while in the heavier isotopomer, nearly instrument limited widths were found. This gives only a lower limit of  $\tau > 800 \text{ ps}$  for  $c_3(1)$  in  $^{15}\text{N}_2$ . Previous time-domain lifetime measurements [18] give similar results:  $170 \pm 30$  and  $1000 \pm 100 \text{ ps}$  for  $^{14}\text{N}_2$  and  $^{15}\text{N}_2$ , respectively, showing that this level in  $^{15}\text{N}_2$  is indeed one of the longest lived singlet *ungerade* states in  $\text{N}_2$  in the region below

Table 3  
Experimentally observed lifetimes  $\tau$  in the isotomers  $^{14}\text{N}_2$  and  $^{15}\text{N}_2$

Level	$^{14}\text{N}_2$		$^{14}\text{N}^{15}\text{N}$	$^{15}\text{N}_2$	
	$\tau$ (ps) obs.	$\tau$ (ps) previous	$\tau$ (ps) previous	$\tau$ (ps) obs.	$\tau$ (ps) previous
$b^1\Pi_u(v=9)$		$\leq 50\text{--}110$ [18]		$46 \pm 7$	
$b^1\Pi_u(v=10)$	$100 \pm 15$				
$c_3^1\Pi_u(v=1)$	$155 \pm 30$	$170 \pm 30$ [18] $230^a$ [16]		$>800$	$1000 \pm 100$ [18]
$c_3^1\Pi_u(v=2)$	$62 \pm 10$				
$o^1\Pi_u(v=1)$		$\leq 50\text{--}110$ [18]		$27 \pm 6$	
$c_4^1\Sigma_u^+(v=1)$	$270 \pm 70$	$330 \pm 35$ [19]	$240 \pm 35$ [19]	$310 \pm 80$	$530 \pm 50$ [18]
$c_4^1\Sigma_u^+(v=2)$	$530 \pm 150$	$675 \pm 50$ [19] $650$ [20]			
$b^1\Sigma_u^+(v=4)$	$160 \pm 70$				
$b^1\Sigma_u^+(v=5)$		$210 \pm 25$ [10] $280$ [20]		$250 \pm 80$	
$b^1\Sigma_u^+(v=6)$	$60 \pm 10$			$55 \pm 10$	

The lifetimes are compared with literature data. All data typically pertain to rotational levels  $J \leq 5$ .

<sup>a</sup> Lifetime for  $J=1$ , see [18] for more information.

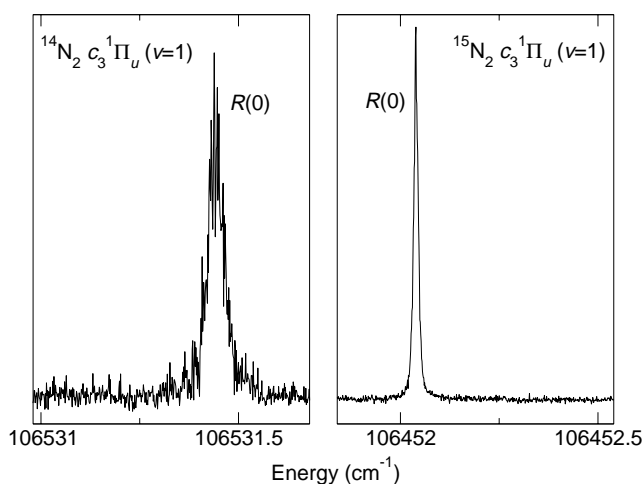


Fig. 3. Isotope dependent width of the  $c_3^1\Pi_u - X^1\Sigma_g^+(1,0)$   $R(0)$  line. Left spectrum:  $^{14}\text{N}_2$ ; line is lifetime broadened. Right spectrum:  $^{15}\text{N}_2$ ; width is nearly instrument limited.

$112000\text{ cm}^{-1}$ . Obviously, high- $n$  Rydberg states, used in zero-kinetic energy experiments, have much longer lifetimes even into the  $\mu\text{s}$  range [21,22].

Although in a previous direct time-domain pump-probe lifetime study [18] individual rotational lines were unresolved, some evidence of a  $J$ -dependence was found for the lifetime of  $c_3(1)$  in  $^{14}\text{N}_2$ . At higher  $J$  levels a shorter lifetime was observed but no accurate lifetime determination could be performed. Kawamoto et al. [16] also investigated this level in  $^{14}\text{N}_2$  by measuring line-widths in the  $c - d''(1,0)$  band and found a decrease in the lifetime with  $J$ : 230 ps at  $J=1$  and 37 ps at  $J=8$  (see for more information [18]).

The  $c_3(2)$  level was measured for  $^{14}\text{N}_2$  yielding a lifetime of  $62 \pm 10$  ps, about two times smaller than that of  $c_3(1)$  in  $^{14}\text{N}_2$ . The  $o^1\Pi_u(v=1)$  Rydberg level was studied in  $^{15}\text{N}_2$  resulting in a lifetime of  $27 \pm 6$  ps. For the latter two states no previous results have been reported.

### 3.2.2. $^1\Sigma_u^+$ states

Two states of  $^1\Sigma_u^+$  symmetry were investigated, the  $c_4^1\Sigma_u^+$  Rydberg state and the  $b^1\Sigma_u^+$  valence state. For  $c_4^1(1)$ , lifetimes of  $270 \pm 70$  and  $310 \pm 80$  ps were derived for  $^{14}\text{N}_2$  and  $^{15}\text{N}_2$ , respectively, showing no significant isotope dependence at the present level of accuracy. Time-domain pump-probe lifetime measurements give lifetimes of  $330 \pm 35$  ps [19] and  $530 \pm 50$  ps [18] for  $^{14}\text{N}_2$  and  $^{15}\text{N}_2$ , respectively. The  $^{14}\text{N}_2$  results agree well, while for  $^{15}\text{N}_2$  differing results are found from line-broadening and pump-probe techniques. We cannot provide a definite explanation for this discrepancy. However, in the pump-probe experiment the bandwidth of the laser is rather limited, to an effect that for  $^{15}\text{N}_2$  some high  $J$  lines in the  $c_3 - X(1,0)$  band are excited when probing  $c_4^1(1)$ . Meanwhile, it has been established that the lifetime for  $c_3(1)$  in  $^{15}\text{N}_2$  is as long as  $1000 \pm 100$  ps [18], hence even a small signal admixture from these longer-lived states could affect the lifetime observed for  $c_4^1(1)$  in  $^{15}\text{N}_2$ . In the present line-broadening study singly-resolved rotational levels are studied. In addition, we note that in the current study similar lifetimes were observed for  $c_4^1(1)$  in  $^{14}\text{N}_2$  and  $^{15}\text{N}_2$ . Since the lifetime of  $c_4^1(1)$  in  $^{14}\text{N}^{15}\text{N}$  is in the same range ( $240 \pm 35$  ps [19]), it may be deduced that for this particular state there is no isotope dependence.

A value of  $530 \pm 150$  ps was determined for the lifetime of the  $c_4^1(2)$  level in  $^{14}\text{N}_2$ . Only a small broadening was observed compared to the instrument width, causing a large uncertainty in the lifetime determination. The present technique is applicable for lifetimes lower than  $\sim 800$  ps, but lifetimes longer than 400 ps are determined more accurately using time-domain pump-probe experiments as have been performed in Lund [18,19,23]. In view of the relatively high uncertainty in the present lifetime of  $c_4^1(2)$ , there is still reasonable agreement with previous data:  $675 \pm 50$  [19] and 650 ps [20].

For the  $b^1\Sigma_u^+$  state, lifetimes of the  $v=4\text{--}6$  vibrational levels were determined. For the  $b^1(4)$  level, here only studied

in  $^{14}\text{N}_2$ , a lifetime of  $160 \pm 70$  ps was obtained. Ubachs et al. [19] assumed a lifetime of 60–80 ps for  $b'(4)$  to explain the lifetime of  $c'_4(1)$  in a Rydberg-valence mixing perturbation model, which seems to be a reasonable estimate. The lifetime of  $b'(5)$  in  $^{14}\text{N}_2$  was already measured with the same setup [10], giving a value of  $210 \pm 25$  ps, not too far off from a value of 280 ps measured by Oertel et al. [20]. In the present study, a lifetime of this level in  $^{15}\text{N}_2$  of  $250 \pm 80$  ps was obtained, hence showing no isotope dependence. Similarly for  $b'(6)$ , no difference in lifetime of the isotopomers was found, with lifetimes of  $60 \pm 10$  and  $55 \pm 10$  ps in  $^{14}\text{N}_2$  and  $^{15}\text{N}_2$ , respectively. The lifetime of  $b'(6)$  is certainly shorter than those of  $b'(4)$  and  $b'(5)$ .

#### 4. Discussion and conclusions

Lifetimes of singlet *ungerade* states between  $106\,000$ – $109\,000$   $\text{cm}^{-1}$  in  $^{14}\text{N}_2$  and  $^{15}\text{N}_2$  have been determined experimentally from linewidth measurements in the frequency domain. The lifetimes provide information about the predissociation rates and for virtually all excited states in  $\text{N}_2$  in the region below  $112\,000$   $\text{cm}^{-1}$ , predissociation dominates radiative decay; for high- $n$  Rydberg states the situation is known to be different [21,22]. In the present study, lifetimes are found to depend on vibrational level and for the  $c_3^1\Pi_u(v=1)$  level also on isotope. Using the coupled-channel Schrödinger equation (CSE) technique, Lewis et al. [5] combined the  $(b,c_3,o)^1\Pi_u$  and  $(C,C')^3\Pi_u$  states in a five-channel CSE model, including all the electrostatic and spin-orbit interactions, to explain the predissociation of the  $b^1\Pi_u(v=0-6)$  and  $c_3^1\Pi_u(v=0)$  states. For these  $^1\Pi_u$  states the predissociation is governed by the  $(C,C')^3\Pi_u$  states. To extend their model on the  $^{1,3}\Pi_u$  states to higher energies, i.e., to the region of the states studied here, more information on the  $^3\Pi_u$  manifold is necessary. Recent rotationally resolved experiments on the  $F^3\Pi_u$  [6] and  $G^3\Pi_u$  [7] states are valuable since the  $F$  and  $G$  states play a significant role at these energies.

A comprehensive predissociation model including singlets and triplets, as was reported for the states of  $^1\Pi_u$  symmetry [5], is not yet developed for the  $^1\Sigma_u^+$  states. However, Ubachs et al. [19] explained lifetimes of  $c'_4^1\Sigma_u^+(v=0-2)$  in  $^{14}\text{N}_2$  from a perspective of Rydberg-valence mixing in the  $^1\Sigma_u^+$  manifold. The pure  $c'_4$  Rydberg state is assumed to be unpredissociated, while Rydberg-valence mixing with the predissociating  $b'$  valence state (possibly by coupling with triplet states) shortens the lifetimes of the Rydberg state levels. For example for the specific level  $c'_4(1)$ , Ubachs et al. showed that this level is strongly mixed with the  $b'$  state with a dominant  $b'(4)$  admixture and assuming a lifetime of 60–80 ps for  $b'(4)$ , they explained the shortening of an estimated radiative lifetime of 740 ps to their observed  $c'_4(1)$  lifetime of 330 ps. Their assumed  $b'(4)$  lifetime is not that far off from the present  $b'(4)$  result of  $160 \pm 70$  ps.

In general, the dependence of the lifetime behaves in a seemingly erratic way for the manifolds of  $^1\Sigma_u^+$  and  $^1\Pi_u$

symmetry. However, comprehensive perturbation models involving singlet and triplet states are able to explain the lifetimes, as was demonstrated by Lewis et al. [5] for a number of  $^1\Pi_u$  states in the limited energetic range below  $106\,000$   $\text{cm}^{-1}$ . Such models should be extended now to include  $^1\Pi_u$  states at higher energies and  $^1\Sigma_u^+$  states. The presently obtained lifetimes can be used as key inputs for these levels.

#### Acknowledgments

The Molecular Atmospheric Physics (MAP) program of the Netherlands Foundation for Research of Matter (FOM) is gratefully acknowledged for financial support. J. Philip is thanked for assistance during the measurements and B.R. Lewis and K.G.H. Baldwin for helpful discussions.

#### References

- [1] D. Stahel, M. Leoni, K. Dressler, J. Chem. Phys. 79 (1983) 2541.
- [2] D. Spelsberg, W. Meyer, J. Chem. Phys. 115 (2001) 6438.
- [3] J.P. Sprengers, W. Ubachs, K.G.H. Baldwin, B.R. Lewis, W.-ÜL. Tchchang-Brillet, J. Chem. Phys. 119 (2003) 3160.
- [4] J.P. Sprengers, W. Ubachs, K.G.H. Baldwin, J. Chem. Phys. 122 (2005) 144301.
- [5] B.R. Lewis, S.T. Gibson, W. Zhang, H. Lefebvre-Brion, J.-M. Robbe, J. Chem. Phys. 122 (2005) 144302.
- [6] J.P. Sprengers, E. Reinhold, W. Ubachs, K.G.H. Baldwin, B.R. Lewis, J. Chem. Phys. 123 (2005) 144315.
- [7] T. Hashimoto, H. Kanamori, submitted (2005).
- [8] S. Hannemann, U. Hollenstein, E.-J. van Duijn, W. Ubachs, Opt. Lett. 30 (2005) 1494.
- [9] M. Sommovilla, Ph.D. Thesis, Diss. ETH Nr. 15688, ETH Zürich (2004).
- [10] J. Philip, J.P. Sprengers, P. Cacciani, C.A. de Lange, W. Ubachs, Appl. Phys. B. 78 (2004) 737.
- [11] K. Yoshino, Y. Tanaka, P.K. Carroll, P. Mitchell, J. Mol. Spectrosc. 54 (1975) 87.
- [12] Harvard-Smithsonian Center for Astrophysics Molecular Database (<http://cfa-www.harvard.edu/amdata/ampdata/N2ARCHIVE/n2home.html>).
- [13] P.K. Carroll, C.P. Collins, Can. J. Phys. 47 (1969) 563.
- [14] P.K. Carroll, C.P. Collins, K. Yoshino, J. Phys. B. 3 (1970) L127.
- [15] K. Yoshino, D.E. Freeman, Y. Tanaka, J. Mol. Spectrosc. 76 (1979) 153.
- [16] Y. Kawamoto, M. Fujitake, N. Ohashi, J. Mol. Spectrosc. 185 (1997) 330.
- [17] W. Ubachs, K.S.E. Eikema, W. Hogervorst, Appl. Phys. B. 57 (1993) 411.
- [18] J.P. Sprengers, A. Johansson, A. L'Huillier, C.-G. Wahlström, B.R. Lewis, W. Ubachs, Chem. Phys. Lett. 389 (2004) 348.
- [19] W. Ubachs, R. Lang, I. Velchev, W.-ÜL. Tchchang-Brillet, A. Johansson, Z.S. Li, V. Lokhnygin, C.-G. Wahlström, Chem. Phys. 270 (2001) 215.
- [20] H. Oertel, M. Kratzat, J. Imschweiler, T. Noll, Chem. Phys. Lett. 82 (1981) 552.
- [21] F. Merkt, S.R. Mackenzie, T.P. Softley, J. Chem. Phys. 103 (1995) 4509.
- [22] R. Seiler, U. Hollenstein, G.M. Greetham, F. Merkt, Chem. Phys. Lett. 346 (2001) 201.
- [23] J.P. Sprengers, W. Ubachs, A. Johansson, A. L'Huillier, C.-G. Wahlström, R. Lang, B.R. Lewis, S.T. Gibson, J. Chem. Phys. 120 (2004) 8973.